Journal of Sound and Vibration (1998) **214**(2), 227–244
Article No. sv971557

OPTIMAL DESIGN BY USING VARIOUS SOLUTIONS FOR VIBRATION OF LAMINATED SHALLOW SHELLS ON SHEAR DIAPHRAGMS

Y. NARITA

Department of Mechanical Engineering, *Hokkaido Institute of Technology*, 7–15 *Maeda*, *Teine*, *Sapporo* 006, *Japan*

AND

T. NITTA

Graduate School, *Hokkaido Institute of Technology*, 7–15 *Maeda*, *Teine*, *Sapporo* 006, *Japan*

(*Received* 16 *July* 1997, *and in final form* 30 *December* 1997)

Free vibration and corresponding optimal design problems are solved for laminated composite shallow shells of rectangular planform. The shells have symmetric laminated construction and are supported by shear diaphragms along the edges. The first-order transverse shear deformation is assumed in the Donnell type shell theory to account for the thickness shear effect, and an analytical solution is presented which is exact for cross-ply laminates and is approximate for angle-ply laminates. A simplified formula is also derived by neglecting inplane inertia terms. Analytical solutions with/without the inplane inertia terms from the classical thin shell theory are also shown. In numerical examples, natural frequencies are presented for various types of shell curvature, e.g., circular cylindrical, spherical and hyperbolic paraboloidal shells. Fibre orientation angles, which cause the maximized fundamental frequencies of the alternating angle-ply shells, are determined, and effects of using the four different vibration solutions are discussed on the optimal frequencies and fibre orientation angles. Questions of how the different solutions quantitatively affect the optimal design results and which solution is recommended in the present type of optimization problems are clarified in the conclusions.

1. INTRODUCTION

Fibrous composite materials are increasingly being used in many weight-sensitive structural applications, which are typically exposed to severe vibration environments. Laminated plate and shell components are quite often encountered among these applications. Accompanying this technical trend has been a growth in the recent literature on vibrations of laminated plates and shells. Even when one limits the search to recent literature in the 1990s, there can be found a considerable number of papers dealing with analyses of laminated flat plates [1–12], and a detailed literature survey was given in references [5, 6] with emphasis on the thick plate analysis.

As for vibration of laminated shallow shells, some recent references can be found [13–21]. Notable work among them is a reference [13] in which a complete and consistent theory is studied to derive equations thoroughly for elastic deformation problems. It seems, however, that accurate comprehensive numerical results are still needed on natural

0022–460X/98/270227 + 18 $30.00/0

frequencies of laminated shallow shells, e.g., the shell with edges constrained by shear diaphragms.

On the other hand, optimal design of laminated plate and shell components is desirable to realize the full potential of fibre reinforced materials. The overall structural performance can be improved by choosing the fibre oreintation angles as design variables, and determining the angles to maximize an object function, typically the fundamental frequency in the vibration problems. A few publications are found for *plate* optimization, e.g., by Fukunaga *et al*. [22] and Grenestedt [23].

Much less has been done to study optimization of *shell* components. Raouf [24] discussed the effects of varying fibre orientation angles on linear and non-linear frequencies of composite panels. Mota Soares *et al*. [25] presented a two-level design approach to deal with composite plate/shell structures by sequentially using the DFP (Davidon–Fletcher–Powell) method. The present first author formulated an analytically oriented design method [26] and employed a genetic algorithm [27] to solve the problem of thin shallow shells supported by shear diaphragms. But these previous studies are limited to the use of the classical theory where thickness shear effects are ignored, and scanty literature is available in which the shear deformation theory is used in the structural analysis part of the optimization.

In the shallow shell theory where the Donnell-type assumption is used [13], an exact solution is obtainable for a single layer, specially orthotropic shell and a cross-ply laminated shell, both supported by shear diaphragms. This solution can also be extended to a sufficiently accurate, approximate solution for a balanced angle-ply shell when the number of layers is large enough to allow for neglecting cross-elasticity stiffness (usually denoted by D_{16}, D_{26}) in bending.

The first objective of this paper is to tabulate the natural frequencies of laminated shallow shells obtained by applying the first-order shear deformation shell theory (FSDST) and the classical shell theory (CST), and also by using reduced solutions with some inertia terms neglected. The influence of using various solutions are discussed for a wide range of curvature and thickness ratio.

The second objective, which is more emphasized in the present paper, is to determine the optimal fibre orientation angles which maximize the fundamental frequencies of the shells by using the four different solutions. Discrepancies among the optimal fibre orientation angles, caused by using the different solutions, are clarified for angle-ply laminated shells having various curvatures and thickness ratios, and some recommendations are made in the choice of vibration solutions when one deals with optimization of shallow shell structures.

2. SOLUTIONS FROM SHEAR DEFORMATION AND CLASSICAL THEORIES

Figure 1 shows a shallow shell bounded by a rectangular planform $a \times b$. The shell has a quadratic middle surface with relatively small, principal constant curvatures $1/Rx$ and $1/Ry$ (Rx and Ry: curvature radii) but no twisting curvature ($1/Rxy = 0$), and has a constant thickness h. A symmetric laminate is considered and therefore the coupling stiffnesses B_{ij} vanish ($B_{ij} = 0$). For cross-ply laminates (i.e., laminates stacked only with 0° and/or 90° piles), the cross-elasticity terms are zero ($A_{16} = A_{26} = D_{16} = D_{26} = 0$), and these terms are assumed in the present study to vanish for angle-ply shells by considering a relatively large number of balanced angle-ply laminates. The u^*, v^* and w^* denote displacements of an arbitrary point in the x, y and z directions, respectively, and u, v and w are those of a point on the middle surface. ρ is the mean mass per unit area of the shell.

2.1. SOLUTION FROM THE FIRST-ORDER SHEAR DEFORMATION THEORY

The Kirchhoff assumption, normally used for the analysis of thin shells, ignores the transverse shear deformation. In contrast, the first-order shear deformation shell theory (FSDST) assumes that normals to the middle surface still remain straight but no longer normal to the surface during deformation. This assumption during deformation is expressed in the shallow shell theory as

$$u^*(x, y, z, t) = u(x, y, t) + z\Phi_x(x, y, t),$$
$$v^*(x, y, z, t) = v(x, y, t) + z\Phi_y(x, y, t),$$
$$w^*(x, y, z, t) = w(x, y, t), \tag{1}$$

by neglecting terms with z/Rx and z/Ry, where ϕ_x and ϕ_y are the rotations of the normals to the middle surface due to bending. Substitution of equations (1) into the linear strain–displacement relations [13] yields

$$\varepsilon_x^*(x, y, z, t) = \frac{\partial u^*}{\partial x} + \frac{w}{R_x} = \frac{\partial u}{\partial x} + z\frac{\partial \Phi_x}{\partial x} + \frac{w}{R_x},$$

$$\varepsilon_y^*(x, y, z, t) = \frac{\partial v^*}{\partial y} + \frac{w}{R_y} = \frac{\partial v}{\partial y} + z\frac{\partial \Phi_y}{\partial y} + \frac{w}{R_y},$$

$$\gamma_{xy}^*(x, y, z, t) = \frac{\partial u^*}{\partial y} + \frac{\partial v^*}{\partial x} = \frac{\partial u}{\partial y} + \frac{\partial v}{\partial x} + z\left(\frac{\partial \Phi_x}{\partial y} + \frac{\partial \Phi_y}{\partial x}\right),$$

$$\gamma_{yz}^* = \frac{\partial v^*}{\partial z} + \frac{\partial w^*}{\partial y} = \Phi_y + \frac{\partial w}{\partial y}, \qquad \gamma_{zx}^* = \frac{\partial u^*}{\partial z} + \frac{\partial w^*}{\partial x} = \Phi_x + \frac{\partial w}{\partial x}$$

The stress–strain relations in the kth layer are given by

$$\begin{Bmatrix} \sigma_1^* \\ \sigma_2^* \\ \tau_{12}^* \end{Bmatrix}^{(k)} = \begin{bmatrix} Q_{11} & Q_{12} & 0 \\ Q_{12} & Q_{22} & 0 \\ 0 & 0 & Q_{66} \end{bmatrix}^{(k)} \begin{Bmatrix} \varepsilon_1^* \\ \varepsilon_2^* \\ \gamma_{12}^* \end{Bmatrix}, \qquad \begin{Bmatrix} \tau_{23}^* \\ \tau_{31}^* \end{Bmatrix}^{(k)} = \begin{bmatrix} Q_{44} & 0 \\ 0 & Q_{55} \end{bmatrix}^{(k)} \begin{Bmatrix} \gamma_{23}^* \\ \gamma_{31}^* \end{Bmatrix}, \tag{3}$$

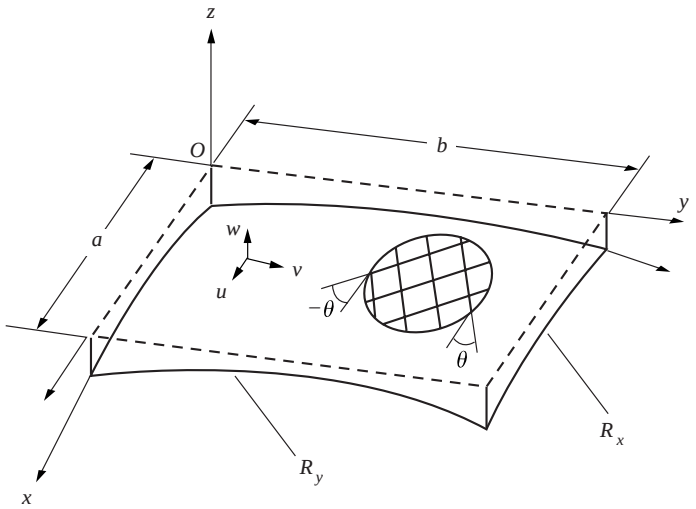

Figure 1. Laminated shallow shell and co-ordinate system.

where the 1 and 2 axes denote major and minor material principal axes, respectively, in the plane and the 3 axes coincide with the z-axis. The material constants Q_{ij} are

$$Q_{11} = \frac{E_1}{1 - \nu_{12}\nu_{21}}, \qquad Q_{22} = \frac{E_2}{1 - \nu_{12}\nu_{21}}, \qquad Q_{12} = \frac{\nu_{12}E_2}{1 - \nu_{12}\nu_{21}},$$

$$Q_{66} = G_{12}, \qquad Q_{44} = G_{23}, \qquad Q_{55} = G_{12} \qquad \text{(superscript } k \text{ is omitted)}, \tag{4}$$

where E_1 and E_2 are moduli of elasticity and G_{12} and G_{23} are shear moduli. The ν_{12} is a Poisson's ratio, which satisfies a reciprocal relation of $E_2\nu_{12} = E_1\nu_{21}$. Equations (3) are converted into the stress–strain relations with respect to the x and y axes [28] as

$$\begin{Bmatrix} \sigma_x^* \\ \sigma_y^* \\ \tau_{xy}^* \end{Bmatrix}^{(k)} = \begin{bmatrix} \bar{Q}_{11} & \bar{Q}_{12} & \bar{Q}_{16} \\ \bar{Q}_{12} & \bar{Q}_{22} & \bar{Q}_{26} \\ \bar{Q}_{16} & \bar{Q}_{26} & \bar{Q}_{66} \end{bmatrix}^{(k)} \begin{Bmatrix} \varepsilon_x^* \\ \varepsilon_y^* \\ \gamma_{xy}^* \end{Bmatrix}, \qquad \begin{Bmatrix} \tau_{yz}^* \\ \tau_{zx}^* \end{Bmatrix}^{(k)} = \begin{bmatrix} \bar{Q}_{44} & \bar{Q}_{45} \\ \bar{Q}_{45} & \bar{Q}_{55} \end{bmatrix}^{(k)} \begin{Bmatrix} \gamma_{yz}^* \\ \gamma_{zx}^* \end{Bmatrix}. \tag{5}$$

When effects of the terms z/Rx and z/Ry are neglected in the usual practice of shallow shell approximation, the stress resultants and moments are obtained by integrating stresses over the thickness

$$\begin{Bmatrix} N_x \\ N_y \\ N_{xy} \end{Bmatrix} = \int_{-h/2}^{h/2} \begin{Bmatrix} \sigma_x^* \\ \sigma_y^* \\ \tau_{xy}^* \end{Bmatrix} \mathrm{d}z, \qquad \begin{Bmatrix} M_x \\ M_y \\ M_{xy} \end{Bmatrix} = \int_{-h/2}^{h/2} \begin{Bmatrix} \sigma_x^* \\ \sigma_y^* \\ \tau_{xy}^* \end{Bmatrix} z \, \mathrm{d}z, \qquad \begin{Bmatrix} Q_y \\ Q_x \end{Bmatrix} = \kappa \int_{-h/2}^{h/2} \begin{Bmatrix} \tau_{yz}^* \\ \tau_{zx}^* \end{Bmatrix} \mathrm{d}z, \tag{6}$$

where κ is a shear correction factor which accounts for the fact that shear stresses are not uniform in the thickness direction [28]. The value of κ is usually taken to be $5/6$ or $\pi^2/12$ for isotropic cases, but in composites it depends on constituent layer properties, fibre orientation angles and so on. For the purpose of numerical study, $\kappa = 5/6$ is used throughout in the present study. Equations (6) are substituted into the equilibrium equations

$$\frac{\partial N_x}{\partial x} + \frac{\partial N_{xy}}{\partial y} = \rho \frac{\partial^2 u}{\partial t^2}, \qquad \frac{\partial N_{xy}}{\partial x} + \frac{\partial N_y}{\partial y} = \rho \frac{\partial^2 v}{\partial t^2}$$

$$\frac{\partial Q_x}{\partial x} + \frac{\partial Q_y}{\partial y} - \frac{N_x}{R_x} - \frac{N_y}{R_y} = \rho \frac{\partial^2 w}{\partial t^2},$$

$$\frac{\partial M_x}{\partial x} + \frac{\partial M_{xy}}{\partial y} - Q_x = \frac{\rho h^3}{12} \frac{\partial^2 \Phi_x}{\partial t^2},$$

$$\frac{\partial M_{xy}}{\partial x} + \frac{\partial M_y}{\partial y} - Q_y = \frac{\rho h^3}{12} \frac{\partial^2 \Phi_y}{\partial t^2}. \tag{7}$$

Then the following governing equations are derived.

$$\begin{Bmatrix} L_{11} & L_{12} & L_{13} & 0 & 0 \\ L_{12} & L_{22} & L_{23} & 0 & 0 \\ L_{13} & L_{23} & L_{33} & L_{34} & L_{35} \\ 0 & 0 & L_{34} & L_{44} & L_{45} \\ 0 & 0 & L_{35} & L_{45} & L_{55} \end{Bmatrix} \begin{Bmatrix} u \\ v \\ w \\ \Phi_x \\ \Phi_y \end{Bmatrix} + \begin{Bmatrix} -\rho & 0 & 0 & 0 & 0 \\ 0 & -\rho & 0 & 0 & 0 \\ 0 & 0 & \rho & 0 & 0 \\ 0 & 0 & 0 & I & 0 \\ 0 & 0 & 0 & 0 & I \end{Bmatrix} \frac{\partial^2}{\partial t^2} \begin{Bmatrix} u \\ v \\ w \\ \Phi_x \\ \Phi_y \end{Bmatrix} = 0, \tag{8}$$

where $I = \rho h^2/12$ is a rotational inertia per unit area of the shell, and the elements L_{ij} in equation (8) are differential operators given by

$$L_{11} = A_{11}\frac{\partial^2}{\partial x^2} + A_{66}\frac{\partial^2}{\partial y^2}, \qquad L_{12} = (A_{12} + A_{66})\frac{\partial^2}{\partial x\,\partial y},$$

$$L_{13} = \left(\frac{A_{11}}{R_x} + \frac{A_{12}}{R_y}\right)\frac{\partial}{\partial x}, \qquad L_{22} = A_{66}\frac{\partial^2}{\partial x^2} + A_{22}\frac{\partial^2}{\partial y^2},$$

$$L_{23} = \left(\frac{A_{12}}{R_x} + \frac{A_{22}}{R_y}\right)\frac{\partial}{\partial y},$$

$$L_{33} = -\kappa\left(A_{55}\frac{\partial^2}{\partial x^2} + A_{44}\frac{\partial^2}{\partial y^2}\right) + \left(\frac{A_{11}}{R_x^2} + 2\frac{A_{12}}{R_x R_y} + \frac{A_{22}}{R_y^2}\right),$$

$$L_{34} = -\kappa A_{55}\frac{\partial}{\partial x}, \qquad L_{35} = -\kappa A_{44}\frac{\partial}{\partial y}, \qquad L_{45} = (D_{11} + D_{66})\frac{\partial^2}{\partial x\,\partial y},$$

$$L_{44} = D_{11}\frac{\partial^2}{\partial x^2} + D_{66}\frac{\partial^2}{\partial y^2} - \kappa A_{55},$$

$$L_{55} = D_{22}\frac{\partial^2}{\partial y^2} + D_{66}\frac{\partial^2}{\partial x^2} - \kappa A_{44}. \tag{9}$$

In equations (9), the (inplane) stretching stiffness A_{ij} and (out-of-plane) bending stiffness D_{ij} are defined by

$$A_{ij} = \sum_{k=1}^{K} \overline{Q}_{ij}^{(k)} \quad (z_k - z_{k-1}),$$

$$D_{ij} = \tfrac{1}{3}\sum_{k=1}^{K} \overline{Q}_{ij}^{(k)} \quad (z_k^3 - z_{k-1}^3), \tag{10}$$

where z_k is the distance from the middle surface to the upper surface of the kth layer. As previously mentioned, coupling terms B_{ij} are deleted due to symmetric laminates, and cross-elasticity terms such as A_{16}, A_{26}, D_{16} and D_{26} are also assumed to vanish.

The displacements of the middle surface may be expressed by functions

$$u(x, y, t) = U_{mn}h\cos\frac{m\pi x}{a}\sin\frac{n\pi y}{b}\,\mathrm{e}^{\mathrm{j}\omega t},$$

$$v(x, y, t) = V_{mn}h\sin\frac{m\pi x}{a}\cos\frac{n\pi y}{b}\,\mathrm{e}^{\mathrm{j}\omega t},$$

$$w(x, y, t) = W_{mn}h\sin\frac{m\pi x}{a}\sin\frac{n\pi y}{b}\,\mathrm{e}^{\mathrm{j}\omega t},$$

$$\phi_x(x, y, t) = \phi_{xmn}\cos\frac{m\pi x}{a}\sin\frac{n\pi y}{b}\,\mathrm{e}^{\mathrm{j}\omega t},$$

$$\phi_y(x, y, t) = \phi_{ymn}\sin\frac{m\pi x}{a}\cos\frac{n\pi y}{b}\,\mathrm{e}^{\mathrm{j}\omega t}, \tag{11}$$

where m and n indicate half wavenumbers of the mode shape along the x *and* y axes, respectively, and U_{mn}, V_{mn}, W_{mn}, ϕ_{xmn} and ϕ_{ymn} are unknown constants representing non-dimensional amplitudes. The thickness h is multiplied in the first three functions of equation (11) to make the constants non-dimensional. The functions satisfy the boundary conditions

$$v = w = M_x = N_x = 0 \quad \text{along} \quad x = 0, a,$$
$$u = w = M_y = N_y = 0 \quad \text{along} \quad y = 0, b \tag{12}$$

when the four edges are supported by shear diaphragms.

Substitution of assumed solutions (11) into (8) yields an eigenvalue equation

$$[\mathbf{K}]\{\mathbf{u}\} = \Omega^2[\mathbf{M}]\{\mathbf{u}\}, \tag{13}$$

where $\{\mathbf{u}\} = \{U_{mn}, V_{mn}, W_{mn}, \phi_{xmn}, \phi_{ymn}\}^{\mathrm{T}}$ and the elements in symmetric matrices [**K**] and [**M**] are given by

$$K_{11} = \bar{A}_{11}\bar{m}^2 + \bar{A}_{66}\bar{n}^2, \qquad K_{12} = (\bar{A}_{12} + \bar{A}_{66})\bar{m}\bar{n},$$
$$K_{13} = -(\bar{A}_{11} + \bar{A}_{12}\gamma)\beta\bar{m}, \qquad K_{22} = \bar{A}_{66}\bar{m}^2 + \bar{A}_{22}\bar{n}^2,$$
$$K_{23} = -(\bar{A}_{12} + \bar{A}_{22}\gamma)\beta\bar{n},$$
$$K_{33} = \kappa(\bar{A}_{55}\bar{m}^2 + \bar{A}_{44}\bar{n}^2) + \beta^2(\bar{A}_{11} + 2\bar{A}_{12}\gamma + \bar{A}_{22}\gamma^2),$$
$$K_{34} = \kappa\bar{A}_{55}\bar{m}, \qquad K_{35} = \kappa\bar{A}_{44}\bar{n}, \qquad K_{45} = (\bar{D}_{12} + \bar{D}_{66})\bar{m}\bar{n},$$
$$K_{44} = \bar{D}_{11}\bar{m}^2 + \bar{D}_{66}\bar{n}^2 + \kappa\bar{A}_{55},$$
$$K_{55} = \bar{D}_{22}\bar{n}^2 + \bar{D}_{66}\bar{m}^2 + \kappa\bar{A}_{44}, \tag{14}$$

and

$$M_{11} = M_{22} = M_{33} = 1, \qquad M_{44} = M_{55} = \varepsilon^2/12, \qquad M_{ij} = 0 \quad (i \neq j). \tag{15}$$

Non-dimensional quantities in equations (14) and (15) are introduced by

$$\alpha = \frac{a}{b} \quad \text{(aspect ratio)}, \qquad \beta = \frac{a}{R_x} \quad \text{(degree of curvature)},$$
$$\gamma = \frac{R_x}{R_y} \quad \text{(curvature ratio)}, \qquad \varepsilon = \frac{h}{a} \quad \text{(thickness ratio)},$$
$$\bar{m} = m\pi, \qquad \bar{n} = \alpha n\pi,$$
$$\bar{A}_{ij} = \frac{A_{ij}a^2}{D_0}, \qquad \bar{D}_{ij} = \frac{D_{ij}}{D_0} \quad \text{(non-dimensional stiffness)},$$
$$\Omega^2 = \frac{\rho\omega^2 a^4}{D_0} \quad \text{(non-dimensional frequency parameter)},$$
$$D_0 = \frac{E_2 h^3}{12(1 - \nu_{12}\nu_{21})} \quad \text{(reference stiffness)}. \tag{16}$$

An eigenvalue problem expressed in the 5×5 matrix equation can be easily solved by using standard eigenvalue routines.

When the inplane and rotational inertias are neglected in equation (13), the frequency parameter Ω^2 can be explicitly solved as

$$\Omega^2 = K_{33} + \frac{2K_{12}K_{13}K_{23} - (K_{22}K_{13}^2 + K_{11}K_{23}^2)}{K_{11}K_{22} - K_{12}^2} + \frac{2K_{34}K_{35}K_{45} - (K_{55}K_{34}^2 + K_{44}K_{35}^2)}{K_{44}K_{55} - K_{45}^2}, \quad (17)$$

where K_{ij} are defined as in equations (14). This explicit expression may be useful to apply in the iteration process of optimization, if it is accurate enough.

2.2. SOLUTION FROM THE CLASSICAL THEORY

In the thin shell theory, the famous Kirchhoff assumption is applied, i.e., normals to the middle surface of the undeformed shell remain straight and normal to the surface during deformation. Under this assumption, a complete set of general equations for shallow shells was derived [13] and the following governing equations may be reduced

$$\begin{bmatrix} L_{11} & L_{12} & L_{13} \\ L_{12} & L_{22} & L_{23} \\ L_{13} & L_{23} & L_{33} \end{bmatrix} \begin{Bmatrix} u \\ v \\ w \end{Bmatrix} + \frac{\partial^2}{\partial t^2} \begin{bmatrix} -\rho & 0 & 0 \\ 0 & -\rho & 0 \\ 0 & 0 & \rho \end{bmatrix} \begin{Bmatrix} u \\ v \\ w \end{Bmatrix} = 0, \quad (18)$$

where the elements L_{ij} $(i, j = 1, 2, 3)$ are the differential operators given by equations (9), except for

$$L_{33} = D_{11}\frac{\partial^4}{\partial x^4} + 2(D_{12} + 2D_{66})\frac{\partial^4}{\partial x^2 \partial y^2} + D_{22}\frac{\partial^4}{\partial y^4} + \left(\frac{A_{11}}{R_x^2} + 2\frac{A_{12}}{R_x R_y} + \frac{A_{22}}{R_y^2}\right). \quad (19)$$

The displacements of the middle surface are expressed by the first three functions of equations (11), and likewise they satisfy the boundary conditions (12) for shear diaphragms. Substitution of the assumed solutions into governing equations (18) yields an eigenvalue equation

$$[\mathbf{K}]\{\mathbf{u}\} = \Omega^2\{\mathbf{u}\}, \quad (20)$$

where $\{\mathbf{u}\} = \{U_{mn}, V_{mn}, W_{mn}\}^{\mathrm{T}}$ and the elements K_{ij} $(i, j = 1, 2, 3)$ in a symmetric matrix $[\mathbf{K}]$ are given by equations (14), except for

$$K_{33} = \bar{D}_{11}\bar{m}^4 + 2(\bar{D}_{12} + 2\bar{D}_{66})\bar{m}^2\bar{n}^2 + \bar{D}_{22}\bar{n}^4 + \beta^2(\bar{A}_{11} + 2\bar{A}_{12}\gamma + \bar{A}_{22}\gamma^2). \quad (21)$$

Non-dimensional quantities in the elements are defined by those in equations (16). The explicit solution, obtained by neglecting inplane inertia terms, is given by just droping the last term of the three-term solution (17) as

$$\Omega^2 = K_{33} + \frac{2K_{12}K_{13}K_{23} - (K_{22}K_{13}^2 + K_{11}K_{23}^2)}{K_{11}K_{22} - K_{12}^2}. \quad (22)$$

3. NUMERICAL EXAMPLE AND OPTIMIZATION

3.1. NUMERICAL EXAMPLE

A numerical example demonstrated here is a laminated shallow shell constrained along the entire edges by shear diaphragms, which is composed of orthotropic layers of equal thickness and of the same composite material. A symmetric 12-layered stacking construction is employed for both cross-ply and angle-ply shells, and an alternating balanced sequence of $[(\theta/-\theta)_3]_s$ (s: symmetric) is assumed for the angle-ply case, where θ is a representative fibre angle as illustrated in Figure 1. The shell has a rectangular

planform ($a/b = 1 \sim 2$) including the square shape ($a/b = 1$). The curvature ratio is taken for open shallow shells with circular cylindrical curvature as $R_x/R_y = 0$ ($R_x > 0$, $R_y = \infty$), with spherical curvature as $R_x/R_y = 1$ (R_x, $R_y > 0$), and with hyperbolic paraboloidal curvature as $R_x/R_y = -1$ ($R_x > 0$, $R_y < 0$).

The material considered is a carbon-fibre composite (CFRP) having a relatively large degree of orthotropy ($E_1/E_2 = 15{\cdot}4$). The elastic constants within lamina [28] are: $E_1 = 138$ GPa, $E_2 = 8{\cdot}96$ GPa, $G_{12} = 7{\cdot}1$ GPa and $v_{12} = 0{\cdot}3$. For the shear deformation theories, such as the first-order theory (FSDST), where the transverse shear modulus is required, the material is assumed to be transversely isotropic as

$$G_{23} = E_2/(1 + v_{23}) \quad \text{with } v_3 = 0{\cdot}3.$$

For the laminated shallow shells thus defined, frequency parameters $\Omega = \omega a^2\sqrt{\rho/D_0}$ are calculated and are used in the optimization process. There are four different types of solutions, designated by: F-I solution: First-order shear deformation shell theory (FSDST) with inplane and rotational inertias Included (equation (13)); F-N solution: First-order shear deformation shell theory (FSDST) with inplane and rotational inertias Neglected (equation (17)); C-I solution: Classical (thin) shell theory (CST) with inplane inertia Included (equation (20)); C-N solution: Classical (thin) shell theory (CST) with inplane inertia Neglected (equation (22)). The focus will be on the effects of using the four different solutions on the calculated natural frequencies, as well as those on the maximized fundamental frequencies in the optimal design.

3.2. OPTIMAL DESIGN PROBLEM

An object function is taken to be a frequency parameter Ω for the fundamental mode of the shallow shell. The maximum point of the object function is searched one-dimensionally with respect to a design variable of the fibre orientation angle θ, since the problem is limited to a balanced, alternating angle-ply $[(\theta/-\theta)_3]_s$. Any specific constraint conditions other than $0^\circ \leqq \theta \leqq 90^\circ$ are not imposed on the design variable.

The term "fundamental frequency" indicates the lowest eigenvalue for given conditions. A vibration mode is identified by a pair of integers (m, n), where m and n are the half wavenumbers in assumed solutions. It is noted in the present problem that the fundamental mode is not limited to $(m, n) = (1, 1)$ and may take on other wavenumbers, such as (1, 2) or (2, 1). This tendency is not unusual in the vibration and buckling problems of shells due to the effect of geometric curvatures, and is more vividly seen in closed cylindrical shells.

The present problem is summarized mathematically in the form

$$\begin{aligned} &\text{Find } \theta \\ &\text{to maximize } (\min \Omega_{mn}) \quad (m, n = 1, 2, \ldots) \\ &\text{subject to } 0^\circ \leqq \theta \leqq 90^\circ, \end{aligned} \tag{23}$$

where the second equation implies that a solution point is sought that maximizes the lowest value of Ω_{mn} for all m and n.

As explained in reference [26], a globally maximum solution is not necessarily determined by looking at the frequency curve with a single (m, n). There are two patterns of how the global solution exists; Case (1): the maximum solution exists at a stationary point of the frequency curve with a single (m, n), and Case (2): the maximum solution exists

TABLE 1

Frequency parameters of thin cross-ply shallow shells with square planform ($a/b = 1$, $h/a = 0{\cdot}01$, $[(0/90)_3]_s$)

$\frac{Rx}{Ry}$	$\frac{a}{Rx}$	Solution	(m, n) (1, 1)	(1, 2)	(2, 1)	(2, 2)	(1, 3)	(3, 1)
0	0·2	F–I	71·64	152·1	135·3	185·8	269·8	287·8
		F–N	71·78	152·3	135·4	186·0	270·0	288·0
		C–I	71·66	152·2	135·4	185·9	270·0	288·1
		C–N	71·79	152·3	135·4	186·0	270·1	288·2
	0·5	F–I	146·4	280·6	147·4	225·9	408·8	289·5
		F–N	148·0	282·6	147·9	226·6	410·5	290·0
		C–I	146·4	280·7	147·5	226·0	409·0	289·8
		C–N	148·0	282·6	147·9	226·6	410·5	290·2
1	0·2	F–I	121·0	170·8	185·5	209·9	277·5	324·0
		F–N	121·3	171·1	185·8	210·1	277·8	324·3
		C–I	121·0	170·9	185·6	210·0	277·7	324·3
		C–N	121·3	171·1	185·8	210·2	277·9	324·5
	0·5	F–I	280·8	340·3	347·8	331·8	439·7	470·2
		F–N	285·9	343·2	350·8	333·4	441·8	472·4
		C–I	280·8	340·4	347·9	331·9	440·0	470·5
		C–N	285·9	343·2	350·8	333·4	441·9	472·5
−1	0·2	F–I	44·09	135·6	153·7	177·0	262·5	311·2
		F–N	44·30	135·9	154·1	177·2	262·9	311·6
		C–I	44·31	135·7	153·8	177·0	262·7	311·5
		C–N	44·31	135·9	154·1	177·2	263·0	311·8
	0·5	F–I	43·19	221·8	233·1	176·0	377·9	412·9
		F–N	44·30	224·4	235·8	177·2	380·3	415·5
		C–I	43·23	221·8	233·1	176·1	378·1	413·2
		C–N	44·31	224·4	235·8	177·2	380·4	415·6

at the crossing point of two frequency curves with a pair of different (m, n)'s for example, (1, 1) and (2, 1) or (1, 2) and (2, 1), with an inequality condition

$$\frac{\partial \Omega_{mn}}{\partial \theta} \cdot \frac{\partial \Omega_{m'n'}}{\partial \theta} \leqq 0. \tag{24}$$

In the present optimization process, one-dimensional sequential search with a coarse increment in θ is carried out first for the frequency parameters with $(m, n) \leqq (2, 2)$, and optimal values with more accuracy are obtained by the golden section method.

4. NATURAL FREQUENCIES OF LAMINATED SHALLOW SHELLS

4.1. EXACT FREQUENCIES OF CROSS-PLY SHELLS

Table 1 presents frequency parameters Ω of symmetrically laminated, cross-ply shallow shells with square planform ($a/b = 1$). The lamination sequence is given by $[(0/90)_3]_s$ having relatively thin total thickness ($h/a = 0{\cdot}01$). For three types of the curvature ratios ($R_x/R_y = 0,\ 1,\ -1$) and two degrees of curvature ($a/R_x = 0{\cdot}2,\ 0{\cdot}5$), frequency parameters calculated by the four solutions are tabulated for (m, n) modes with $m + n \leqslant 4$.

It is seen in the table that the C-I and C-N solutions yield greater frequencies than the F-I and F-N solutions, respectively, because fewer degrees of freedom in the solutions give rise to stiffening effects in the system. For the same reason, frequencies without inplane inertia, C-N and F-N, give larger values than those with inertia, C-I and F-I, respectively. Thus, among the four solutions presented, frequencies from the C-N solution are the largest and those from the F-I solution are the smallest values, for each (m, n) mode in the table. Such discrepancies between the two solutions are slightly magnified as the degree of curvature a/R_x increases from 0·2 to 0·5. Among three types of the curvature ratios R_x/R_y, the largest discrepancy of 2·5% is seen in the (1, 1) mode of the hyperbolic paraboloidal shell ($R_x/R_y = -1$), but the others are about 1% or less.

The lamination $[(0/90)_3]_s$ implies that the outer 0° layer of each (0/90) pair has stronger stiffening effect in bending than the inner 90° layer, and this causes greater frequencies of the (2, 1) mode than those of the (1, 2) modes in two types of the curvature ratios ($R_x/R_y = 1,\ -1$). But for the cylindrical shells ($R_x/R_y = 0$), geometrical stiffening in the y direction due to cylindrical curvature has a more dominant effect than the material stiffening in the x direction, and the frequencies of the (1, 2) mode have larger values than the (2, 1) mode with about 12% discrepancy for $a/R_x = 0{\cdot}2$ and even greater, 90% for $a/R_x = 0{\cdot}5$.

Table 2 presents frequency parameters Ω in the same format as Table 1, except that shells are relatively thick ($h/a = 0{\cdot}1$). The other geometric and material parameters are identical to those in Table 1, and the effect of difference in thickness may be extracted. Generally speaking, tendencies observed in using the four different solutions are the same as in Table 1. But discrepancies between the C-N and F-I solutions, which are the largest and smallest for each (m, n), respectively, are magnified to a large extent, and for half of the values presented the discrepancies are even greater than 5%. Also noted is that the frequency parameters are in the order of the C-N, C-I, F-N and F-I solutions descending from the largest C-N solution, except for only three cases of the (1, 1) mode of the three curvature ratios ($R_x/R_y = 0,\ -1$ and 1) with $a/R_x = 0{\cdot}5$ where the order of the C-I and F-N solutions is interchanged.

4.2. APPROXIMATE FREQUENCIES OF ANGLE-PLY SHELLS

Figures 2–5 show variations of frequency parameters Ω, calculated by the F-I solution, with the fibre angle θ for 12-layered, alternating angle-ply laminates $[(\theta/-\theta)_3]_s$. The solid lines denote frequencies of relatively thick shells ($h/a = 0{\cdot}1$) and broken lines, those of thin shells ($h/a = 0{\cdot}01$). The shells have an aspect ratio $a/b = 1$ (square planform) and the degree of curvature is taken to be $a/R_x = 0{\cdot}5$ in each figure, except for Figure 2 dealing with flat plates.

Figure 2 shows frequency parameters of laminated flat plates ($a/R_x = 0$), as a special case of the shallow shell. The frequency variations are exactly symmetric at about $\theta = 45^\circ$, and the discrepancies between two sets of frequencies are small, particularly for the lowest (1, 1) mode. As seen, the fibre angle θ does not have a significant effect on the lowest mode, and the maximum is found at $\theta = 45^\circ$ which is a stationary point of the curve.

Figure 3 considers laminated shells having circular cylindrical curvature ($R_x/R_y = 0$). Although the frequencies are no longer symmetric about at $\theta = 45^\circ$ due to the geometric curvature in one direction ($R_x > 0$, $R_y = \infty$), the variations in frequencies for thick shells (shown by solid lines, $h/a = 0{\cdot}1$) are very similar to those for flat plates. In contrast, the variations of thin shells (shown by broken lines, $h/a = 0{\cdot}01$) appear totally different, giving the maximum of the fundamental frequency at a crossing point of two curves (1, 1) and (2, 1). This difference between two variations indicates that the membrane stiffness effect by the cylindrical geometric curvature is dominant for thin shells ($h/a = 0{\cdot}01$), while bending stiffnesses D_{ij} are magnified by the cube of thickness h, and the larger thickness

TABLE 2

Frequency parameters of thick cross-ply shallow shells with square planform ($a/b = 1$, $h/a = 0{\cdot}1$, $[(0/90)_3]_s$)

$\frac{Rx}{Ry}$	$\frac{a}{Rx}$	Solution	(m, n) (1, 1)	(1, 2)	(2, 1)	(2, 2)	(1, 3)	(3, 1)
0	0·2	F–I	43·92	107·7	127·0	167·4	217·7	262·5
		F–N	44·35	109·9	129·4	172·4	225·4	271·1
		C–I	44·59	111·8	132·9	177·2	234·2	287·7
		C–N	44·67	111·9	133·0	177·3	234·4	287·8
	0·5	F–I	45·34	109·6	126·8	167·5	218·9	262·2
		F–N	46·20	112·5	129·5	172·8	227·6	271·2
		C–I	46·00	113·6	132·7	177·3	235·2	287·3
		C–N	46·50	114·4	133·1	177·8	236·4	287·8
1	0·2	F–I	44·93	108·0	127·5	167·6	217·8	262·8
		F–N	45·41	110·2	130·0	172·6	225·5	271·6
		C–I	45·59	112·0	133·4	177·4	234·3	287·9
		C–N	45·72	112·2	133·6	177·6	234·5	288·2
	0·5	F–I	50·94	111·1	129·8	168·9	219·3	263·6
		F–N	52·27	114·1	133·4	174·6	228·1	273·7
		C–I	51·60	115·0	135·6	178·6	235·7	288·2
		C–N	52·54	116·0	136·8	179·5	237·0	290·2
−1	0·2	F–I	43·46	107·4	127·0	167·2	217·5	262·5
		F–N	43·99	109·7	129·6	172·3	225·4	271·4
		C–I	44·12	111·5	132·9	177·0	234·0	287·6
		C–N	44·30	111·7	133·2	177·2	234·3	288·0
	0·5	F–I	42·57	107·8	126·9	166·3	217·8	262·0
		F–N	43·99	111·1	130·8	172·3	227·0	272·8
		C–I	43·20	111·7	132·6	176·0	234·1	286·5
		C–N	44·31	113·1	134·4	177·2	235·9	289·3

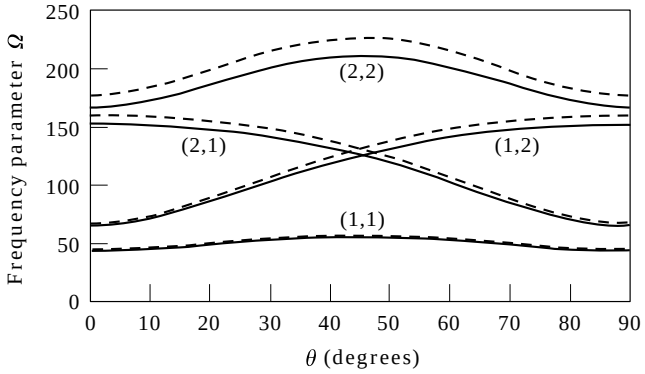

Figure 2. Variations of frequency parameters Ω of 12-layered flat plates versus the fibre angle θ ($a/R_x = 0$, $a/b = 1$, $[(\theta/-\theta)_3]_s$; ——: $h/a = 0{\cdot}1$, – – –: $h/a = 0{\cdot}01$).

($h/a = 0{\cdot}1$) suppresses the membrane effect, eventually resulting in similar frequency variations to the flat plate.

Figure 4 and 5 present the frequencies Ω of spherical and hyperbolic paraboloidal shells, respectively. Both variations are symmetric with respect to $\theta = 45^\circ$ and their patterns of the thick case are again similar to the flat plate for the same reason given for the cylindrical shell. For the thin spherical shells in Figure 4, the maximum fundamental frequency is given at $\theta = 45^\circ$, a crossing point of the (1, 2) and (2, 1) curves. In Figure 5, especially noted is that both fundamental frequencies almost coincide for hyperbolic paraboloidal shells with different thicknesses ($h/a = 0{\cdot}01$ and $0{\cdot}1$), this is a very unique feature of such a shell, which has positive and negative geometric curvature inside the boundary.

5. OPTIMAL FREQUENCIES OF ANGLE-PLY SHALLOW SHELLS

In Tables 3–5, optimal frequency parameters Ω_{opt} are presented, which are maximized with respect to the fibre angle θ for alternating angle-ply $[(\theta/-\theta)_3]_s$ laminated shells. The optimal design variables θ_{opt} and corresponding wavenumbers $(m, n)_{opt}$ are also given for $h/a = 0{\cdot}01$ and $0{\cdot}1$. All these optimal values are calculated by using the four different solutions for three aspect ratios ($a/b = 1, 1{\cdot}5, 2$) and two degrees of curvature ($a/R_x = 0{\cdot}2, 0{\cdot}5$) in each table. A single $(m, n)_{opt}$ represents Case (1): the optimal value is

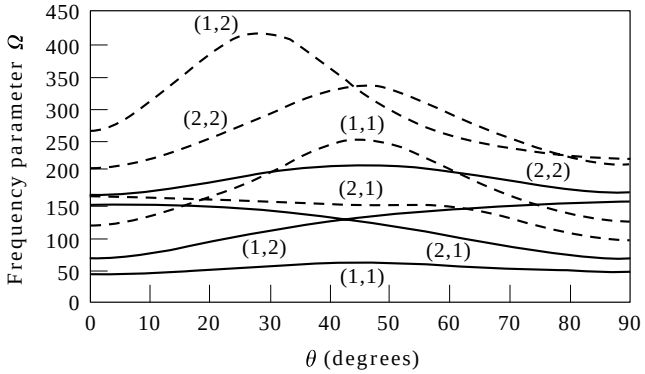

Figure 3. Variations of frequency parameters Ω of 12-layered shallow shells with cylindrical curvature versus the fibre angle θ ($R_x/R_y = 0$, $a/R_x = 0{\cdot}5$, $a/b = 1$, $[(\theta/-\theta)_3]_s$; ——: $h/a = 0{\cdot}1$, – – –: $h/a = 0{\cdot}01$).

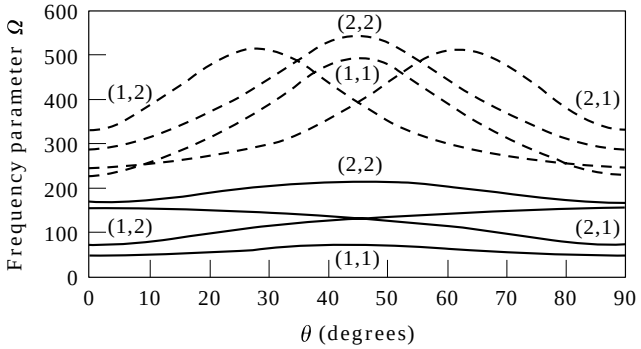

Figure 4. Variations of frequency parameters Ω of 12-layered shallow shells with spherical curvature versus the fibre angle θ ($R_x/R_y = 1$, $a/R_x = 0{\cdot}5$, $a/b = 1$, $[(\theta/-\theta)_3]_s$; ——: $h/a = 0{\cdot}1$, – – –: $h/a = 0{\cdot}01$).

obtained at a stationary point of a frequency curve of this (m, n), while the two $(m, n)_{opt}$'s represent Case (2): the optimal point exists at a crossing point of two frequency curves of these (m, n)'s.

In Table 3, given for the cylindrical curvature ($R_x/R_y = 0$), it is clearly seen among the four solutions that there are practically no discrepancies in the optimal values θ_{opt} and Ω_{opt} for thin shells ($h/a = 0{\cdot}01$). For thick shells ($h/a = 0{\cdot}1$), the discrepancies among the four values in Ω_{opt} are a little intensified and are increased with larger aspect ratio a/b, for example about 5% for a rectangular planform ($a/b = 2$). But again, no significant discrepancies among them are observed on the optimal θ_{opt}. For optimal modes $(m, n)_{opt}$, Case (1) with (1, 1) mode and Case (2) between the (1, 1) and (2, 1) modes are seen for thin shells, while only the (1, 1) mode is obtained for thick shells.

For a square planform ($a/b = 1$), the value of θ_{opt} is nearly equal to 45° for a thin shallow shell ($a/R_x = 0{\cdot}2$, $h/a = 0{\cdot}01$), but the one-dimensional stiffening effect of the cylindrical curvature becomes dominant and yields $\theta_{opt} \fallingdotseq 19^\circ$ for a deeper shell ($a/R_x = 0{\cdot}5$). This curvature effect is, however, diminished yielding again optimal solutions $\theta_{opt} \fallingdotseq 45^\circ$ for thick shells ($h/a = 0{\cdot}1$), because of the bending stiffness increasing with the cube of thickness h.

In Table 4, sets of the optimal results by the four solutions are given for the spherical curvature ($R_x/R_y = 1$). Due to the diagonal symmetry of the square shell ($a/b = 1$), all the optimal fibre angles of the shells are exactly $\theta_{opt} = 45^\circ$, but optimal modes $(m, n)_{opt}$ are

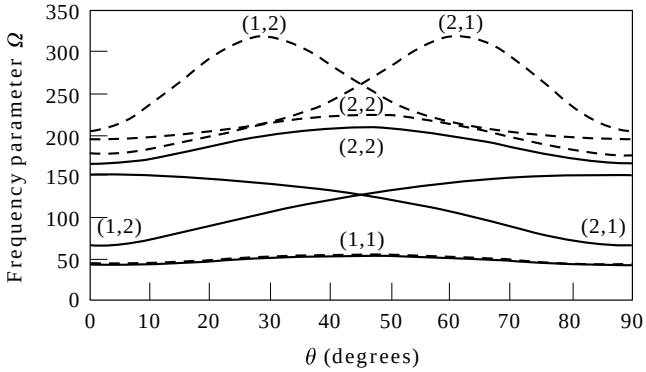

Figure 5. Variations of frequency parameters Ω of 12-layered shallow shells with hyperbolic paraboloidal curvature versus the fibre angle θ ($R_x/R_y = -1$, $a/R_x = 0{\cdot}5$, $a/b = 1$, $[(\theta/-\theta)_3]_s$; ——: $h/a = 0{\cdot}1$, – – –: $h/a = 0{\cdot}01$).

TABLE 3

Optimal frequency parameters of angle-ply shallow shells with cylindrical curvature $(Rx/Ry = 0)$

$\frac{a}{b}$	$\frac{a}{Rx}$	Solution	$h/a = 0{\cdot}01$ θ_{opt}	Ω_{opt}	$(m, n)_{opt}$	$h/a = 0{\cdot}1$ θ_{opt}	Ω_{opt}	$(m, n)_{opt}$
1·0	0·2	F–I	45·1	114·0	(1, 1)	45·3	56·24	(1, 1)
		F–N	45·0	114·1	(1, 1)	45·0	56·76	(1, 1)
		C–I	45·1	114·0	(1, 1)	45·3	57·31	(1, 1)
		C–N	45·0	114·1	(1, 1)	45·0	57·39	(1, 1)
	0·5	F–I	19·5	160·8	(1, 1)(2, 1)	46·3	60·14	(1, 1)
		F–N	18·9	161·6	(1, 1)(2, 1)	45·0	61·14	(1, 1)
		C–I	19·5	160·8	(1, 1)(2, 1)	46·3	61·18	(1, 1)
		C–N	18·9	161·7	(1, 1)(2, 1)	45·0	61·72	(1, 1)
1·5	0·2	F–I	35·7	160·3	(1, 1)	63·7	91·56	(1, 1)
		F–N	35·7	160·4	(1, 1)	63·8	92·70	(1, 1)
		C–I	35·7	160·3	(1, 1)	63·6	94·35	(1, 1)
		C–N	35·7	160·4	(1, 1)	63·6	94·35	(1, 1)
	0·5	F–I	50·7	244·0	(1, 1)	59·5	93·35	(1, 1)
		F–N	50·5	244·8	(1, 1)	59·4	94·54	(1, 1)
		C–I	50·6	244·1	(1, 1)	59·5	96·13	(1, 1)
		C–N	50·5	244·9	(1, 1)	59·4	96·17	(1, 1)
2·0	0·2	F–I	31·0	192·9	(1, 1)	90·0	152·3	(1, 1)
		F–N	30·9	193·0	(1, 1)	90·0	155·1	(1, 1)
		C–I	30·9	193·0	(1, 1)	90·0	160·0	(1, 1)
		C–N	30·9	193·0	(1, 1)	90·0	160·0	(1, 1)
	0·5	F–I	43·9	334·2	(1, 1)(2, 1)	90·0	152·7	(1, 1)
		F–N	43·8	335·0	(1, 1)(2, 1)	90·0	156·0	(1, 1)
		C–I	43·9	334·4	(1, 1)(2, 1)	90·0	160·4	(1, 1)
		C–N	43·8	335·1	(1, 1)(2, 1)	90·0	160·6	(1, 1)

found as Case (2) for the thin shell and Case (1) for the thick shell. It is generally seen in the table that optimal modes $(m, n)_{opt}$ of the thin shells with deep curvature ($h/a = 0{\cdot}01$, $a/R_x = 0{\cdot}5$) fall into Case (2) and $(m, n)_{opt}$ of the thick shells fall into Case (1), without exception.

Table 5 presents the optimal results calculated by the four solutions for the hyperbolic paraboloidal curvature ($R_x/R_y = -1$). The fundamental frequencies for shells of square planform ($a/b = 1$) with different thicknesses exhibit only slight differences, as observed in Figure 5, and naturally the optimal solutions θ_{opt} and Ω_{opt} for $h/a = 0{\cdot}01$ and $0{\cdot}1$ are quite close to each other in the table. But this tendency is seen only for the square planform and is not observed for shells with other aspect ratios.

It is seen, on the whole, in Tables 3–5 that the optimal solutions for thick shells ($h/a = 0{\cdot}1$) are not so sensitive to the difference in the curvature ratios ($R_x/R_y = 0$, 1 and -1), and the values of θ_{opt} and Ω_{opt} are allocated within certain ranges, regardless of the curvature ratio of R_x/R_y, showing the constant optimal mode (1, 1).

6. CONCLUSIONS

The free vibration of laminated shallow shells has been considered by using the first-order shear deformation and the classical thin shell theories. Especially the optimal design problem of the laminated shells was studied to obtain the optimal fibre orientation angles resulting in the largest value of its fundamental frequency. By combining the two

TABLE 4

Optimal frequency parameters of angle-ply shallow shells with spherical curvature ($Rx/Ry = 1$)

			$h/a = 0{\cdot}01$			$h/a = 0{\cdot}1$		
$\frac{a}{b}$	$\frac{a}{Rx}$	Solution	θ_{opt}	Ω_{opt}	$(m, n)_{opt}$	θ_{opt}	Ω_{opt}	$(m, n)_{opt}$
1·0	0·2	F–I	45·0	198·8	(1, 2)(2, 1)	45·0	58·77	(1, 1)
		F–N	45·0	199·2	(1, 2)(2, 1)	45·0	59·30	(1, 1)
		C–I	45·0	198·9	(1, 2)(2, 1)	45·0	59·84	(1, 1)
		C–N	45·0	199·2	(1, 2)(2, 1)	45·0	59·90	(1, 1)
	0·5	F–I	45·0	393·5	(1, 2)(2, 1)	45·0	73·62	(1, 1)
		F–N	45·0	397·0	(1, 2)(2, 1)	45·0	74·70	(1, 1)
		C–I	45·0	393·6	(1, 2)(2, 1)	45·0	74·66	(1, 1)
		C–N	45·0	397·0	(1, 2)(2, 1)	45·0	75·18	(1, 1)
1·5	0·2	F–I	34·9	215·1	(1, 1)	63·2	91·78	(1, 1)
		F–N	35·0	215·3	(1, 1)	63·0	93·06	(1, 1)
		C–I	34·9	215·1	(1, 1)	63·1	94·56	(1, 1)
		C–N	35·0	215·3	(1, 1)	62·8	94·71	(1, 1)
	0·5	F–I	39·1	438·4	(1, 2)(2, 1)	46·0	95·35	(1, 1)
		F–N	39·1	441·0	(1, 2)(2, 1)	47·3	97·82	(1, 1)
		C–I	39·1	438·6	(1, 2)(2, 1)	49·6	97·93	(1, 1)
		C–N	39·1	441·0	(1, 2)(2, 1)	48·7	99·29	(1, 1)
2·0	0·2	F–I	29·7	227·2	(1, 1)	90·0	152·3	(1, 1)
		F–N	29·8	227·5	(1, 1)	90·0	155·1	(1, 1)
		C–I	29·7	227·3	(1, 1)	90·0	160·0	(1, 1)
		C–N	29·8	227·5	(1, 1)	90·0	160·1	(1, 1)
	0·5	F–I	34·6	487·1	(1, 1)(2, 1)	90·0	152·8	(1, 1)
		F–N	34·7	490·0	(1, 1)(2, 1)	90·0	156·1	(1, 1)
		C–I	34·6	487·3	(1, 1)(2, 1)	90·0	160·5	(1, 1)
		C–N	34·7	490·0	(1, 1)(2, 1)	90·0	161·0	(1, 1)

TABLE 5

Optimal frequency parameters of angle-ply shallow shells with hyperbolic paraboloidal curvature $(Rx/Ry = -1)$

			$h/a = 0{\cdot}01$			$h/a = 0{\cdot}1$		
$\frac{a}{b}$	$\frac{a}{Rx}$	Solution	θ_{opt}	Ω_{opt}	$(m, n)_{opt}$	θ_{opt}	Ω_{opt}	$(m, n)_{opt}$
1.0	0·2	F–I	44·2	56·29	(1, 1)	45.0	55.19	(1, 1)
		F–N	45·0	56·52	(1, 1)	45·0	55·89	(1, 1)
		C–I	45·0	56·30	(1, 1)	45·0	56·25	(1, 1)
		C–N	45·0	56·53	(1, 1)	45.0	56.53	(1, 1)
	0·5	F–I	46·2	55·14	(1, 1)	45·0	53·88	(1, 1)
		F–N	45.0	56·52	(1, 1)	45·0	55·89	(1, 1)
		C–I	45.0	55·15	(1, 1)	45.0	54·89	(1, 1)
		C–N	45.0	56·53	(1, 1)	45.0	56·53	(1, 1)
1.5	0·2	F–I	38.5	112·9	(1, 1)	64·1	91.21	(1, 1)
		F–N	38·8	113·1	(1, 1)	64·3	92.47	(1, 1)
		C–I	38·8	112·9	(1, 1)	63.9	93·99	(1, 1)
		C–N	38·8	113·1	(1, 1)	64.0	94·13	(1, 1)
	0·5	F–I	36·0	205·3	(1, 1)(2, 1)	62·6	91·05	(1, 1)
		F–N	36·8	207·4	(1, 1)(2, 1)	63·1	93·00	(1, 1)
		C–I	35·9	205·4	(1, 1)(2, 1)	62·4	93·79	(1, 1)
		C–N	36·8	207·5	(1, 1)(2, 1)	62·9	94·66	(1, 1)
2.0	0·2	F–I	33·8	162·1	(1, 1)	90.0	152·0	(1, 1)
		F–N	33·8	162·2	(1, 1)	90·0	155·0	(1, 1)
		C–I	33·8	162·1	(1, 1)	90·0	159·7	(1, 1)
		C–N	33·8	162·2	(1, 1)	90.0	160·0	(1, 1)
	0·5	F–I	45·3	224·5	(1, 1)(2, 1)	90·0	151·4	(1, 1)
		F–N	45·0	226·0	(1, 1)(2, 1)	90·0	155·4	(1, 1)
		C–I	45·0	224·7	(1, 1)(2, 1)	90·0	159·0	(1, 1)
		C–N	45·0	226·1	(1, 1)(2, 1)	90·0	160·3	(1, 1)

shell theories with/without inplane and rotational inertia effects, four different types of analytical solutions were derived and used to determine optimal fibre orientation angles, frequency parameters and corresponding mode numbers.

In numerical demonstrations, comprehensive sets of frequency parameters were tabulated for the cross-ply laminated shells and were plotted with fibre angles of the angle-ply shells. Optimal solutions were also presented in tables for wide ranges of aspect ratios and degrees of curvature with three typical geometric configurations of cylindrical, spherical and hyperbolic paraboloidal curvatures.

It was observed from the optimal solutions that geometric curvature effects are dominant for thin shells, but become diminished as the shells get thicker. As for effects in using four different solutions, it was concluded from a practical viewpoint that the simplest explicit

solution from the classical shell theory without inplane inertial suffices for the purpose of determining optimal fibre orientation angles with respect to the maximum fundamental frequency. The other more elegant solutions may be required when higher frequencies and other complicating effects are under consideration.

REFERENCES

1. K. Hosokawa, T. Yada and T. Sakata 1993 *JSME International Journal* **36**, 296–300. Free vibrations of symmetrically laminated composite plates.
2. B. Baharlou and A. W. Leissa 1993 *International Journal of Mechanical Sciences* **29**, 545–555. Vibration and buckling of generally laminated composite plates with arbitrary edge conditions.
3. G. B. Chai 1994 *Composite Structures* **29**, 249–258. Free vibration of generally laminated composite plates with various edge support conditions.
4. P. S. Frederiksen 1995 *Journal of Sound and Vibration* **186**, 743–759. Single-layer plate theories applied to the flexural vibration of completely free thick laminates.
5. K. M. Liew, Y. Xiang and S. Kitipornchai 1995 *Journal of Sound and Vibration* **180**, 163–176. Research on thick plate vibration: a literature survey.
6. A. Tessler, E. Saether and T. Tsui 1995 *Journal of Sound and Vibration* **179**, 475–498. Vibration of thick laminated composite plates.
7. C. W. Bert and M. Malik 1996 *Journal of Sound and Vibration* **193**, 927–933. On the relative effects of transverse shear deformation and rotary inertia on the free vibration of symmetric cross-ply laminated plates.
8. C. A. Shankara and N. G. Iyengar 1996 *Journal of Sound and Vibration* **191**, 721–738. A C° element for the free vibration analysis of laminated composite plates.
9. A. A. Khdeir 1995 *Journal of Sound and Vibration* **188**, 257–267. Forced vibration of antisymmetric angle-ply laminated plates with various boundary conditions.
10. D. J. Gorman and W. Ding 1996 *Composite Structures* **34**, 387–395. Accurate free vibration analysis of clamped antisymmetric angle-ply laminated rectangular plates by the superposition-Galerkin method.
11. K. M. Liew 1996 *Journal of Sound and Vibration* **198**, 343–360. Solving the vibration of thick symmetric laminates by Reissner/Mindlin plate theory and the P-Ritz method.
12. J. M. Lee, J. H. Chung and T. Y. Chung 1997 *Journal of Sound and Vibration* **199**, 71–85. Free vibration analysis of symmetrically laminated composite rectangular plates.
13. A. W. Leissa and M. A. Qatu 1991 *Journal of Applied Mechanics* **58**, 181–188. Equations of elastic deformation of laminated composite shallow shells.
14. M. S. Qatu and A. W. Leissa 1991 *Composite Structures* **17**, 227–255. Natural frequencies for cantilevered doubly curved laminated composite shallow shells.
15. A. A. Khdeir and J. N. Reddy 1990 *Computers & Structures* **34**, 817–826. Influence of edge conditions on the modal characteristics of cross-ply laminated shells.
16. L. Chun and K. Y. Lam 1995 *Composite Structures* **30**, 389–397. Dynamic analysis of clamped laminated curved panels.
17. Y. Kobayashi and A. W. Leissa 1995 *International Journal of Nonlinear Mechanics* **30**, 57–66. Large amplitude free vibration of thick shallow shells supported by shear diaphragms.
18. C. W. Lim and K. M. Liew 1994 *Journal of Sound and Vibration* **173**, 343–375. A pb-2 Ritz formulation for flexural vibration of shallow cylindrical shells of rectangular planform.
19. C. W. Lim and K. M. Liew 1995 *International Journal of Mechanical Sciences* **37**, 277–295. A higher order theory for vibration of shear deformable cylindrical shallow shells.
20. C. W. Lim and K. M. Liew 1996 *Journal of the Acoustical Society of America* **100**, 3665–3673. Vibration of moderately thick cylindrical shallow shells.
21. K. M. Liew, C. W. Lim and S. Kitipornchai 1997 *Applied Mechanics Review* **50**, Various theories for vibration of shallow shells: a review with bibliography.
22. H. Fukunaga, H. Sekine and M. Sato 1994 *Journal of Sound and Vibration* **171**, 219–229. Optimal design of symmetric laminated plates for fundamental frequency.
23. S. L. Grenestedt 1989 *Composite Structures* **12**, 193–209. Layup optimization and sensitivity analysis of the fundamental eigenfrequency of composite plates.
24. R. A. Raouf 1994 *Composite Structures* **29**, 259–267. Tailoring the dynamic characteristics of composite panels using fiber orientation.

25. C. M. Mota Soares, V. Franco Correia, H. Mateus and J. Herskovits 1995 *Composite Structures* **30**, 147–157. A discrete model for the optimal design of thin composite plate–shell type structures using a two-level approach.
26. Y. Narita and X. Zhao 1998 *International Journal of Solids and Structures* **35,** 2571–2583. An optimal design for the maximum fundamental frequency of laminated shallow shells.
27. Y. Narita, M. Itoh and X. Zhao 1996 *Advanced Composite Letters* **5**, 21–24. Optimal design by genetic algorithm for maximum fundamental frequency of laminated shallow shells.
28. J. R. Vinson and R. L. Sierakowski 1986 *The Behavior of Structures Composed of Composite Materials*. Dordrecht: Martinus Nijhoff Publishers.